PATH FOLLOWING BI-DIRECTIONAL CONTROLLER FOR ARTICULATED VEHICLES

A. S. TOMAR, MSc, Researcher at HAN University of Applied Sciences

K. KURAL, MEng., MSc, Researcher at HAN University of Applied Sciences, PhD student at Eindhoven University of Technology

R. KUSUMAKAR, MSc, Researcher at HAN University of Applied Sciences

A. NAREN, Graduate student at HAN University of Applied Sciences

Abhishek Singh Tomar [1]), Karel Kural [1]) [2]), Rakshith Kusumakar [1]), Arun Naren [1])

[1]) HAN University of Applied Sciences, Arnhem [2]) Eindhoven University of Technology

PO BOX 2217, Arnhem 6802 CE, The Netherlands
Phone: +31 (0)6 16 419 689
Email: AbhishekSingh.Tomar@han.nl

Abstract

Docking or parking articulated vehicles is a difficult task which further becomes complex with increasing number of articulations, which can be arduous for even professional drivers. Driver's limited view and perception coupled with divergent instability of articulated vehicles in reverse motion are the primary reasons of complexity of the maneuver. For such, a driver support system is developed using a path following controller based on a virtual tractor principle. This paper presents the control problem formulation together with brief descriptions of relevant components of the closed-loop. An optimization routine is also presented which can be used to tune the controller gains. A proof of concept is presented for a single articulated vehicle using simulations and a second proof of concept is demonstrated using scaled test setup, which also indicates that the presented controller can be implemented in full scale vehicle. Due to a generic description presented in this paper, the controller is flexible and can be extended for double articulated vehicles.

Keywords: Path Following Controller, Articulated Vehicles, Low Speed Maneuvering, Bi-directional Controller, Docking maneuver

1. Introduction

Increasing population and demand on transportation of goods are resulting in higher number of vehicles on roads, leading to growing traffic volume and road accidents. High capacity vehicles (HCVs) consisting more than one number of articulations might be a potential solution to this ever increasing demand. HCVs are already operational in Scandinavian countries, The Netherlands, Australia, Canada, USA and South Africa due to their ability to reduce fuel consumption, road wear and traffic congestion, as indicated by Odhams et al. (2010). However, handling and stability aspects of HCVs become more challenging with increasing number of articulations, especially when it concerns the parking or docking of these vehicles.

The complexity of such maneuvers is mainly due to two reasons; one is due to the human driver's perception (visual, vehicle feedback, external feedback) which is limited to the field-view of side mirrors while reversing and the presence of articulation makes it strenuous even for professional drivers as investigated by Rakic et al. (2011) and the second is due to the inheritance divergent instability of articulated vehicles in reverse motion.

A typical docking or parking maneuver for HCVs contain both forward and reverse motion phases as schematically presented in Figure 1(a). A top view of semitrailer at docking gate is schematically presented in Figure 1(b) to indicate the lateral error tolerance te_y which is set by the spacing of docking rails (approx. 2.6-2.7 [m]) and the orientation error tolerance te_θ is by the width of cargo and docking gate. It can also be observed that with the presence of orientation error at docking gate, the lateral error tolerance will further decrease. Due to these physical limitations at the docking gates together with the human driver's limited view and perception, docking rails and gates get damaged during the maneuver and can be found at several distribution centers, which results in additional maintenance cost.

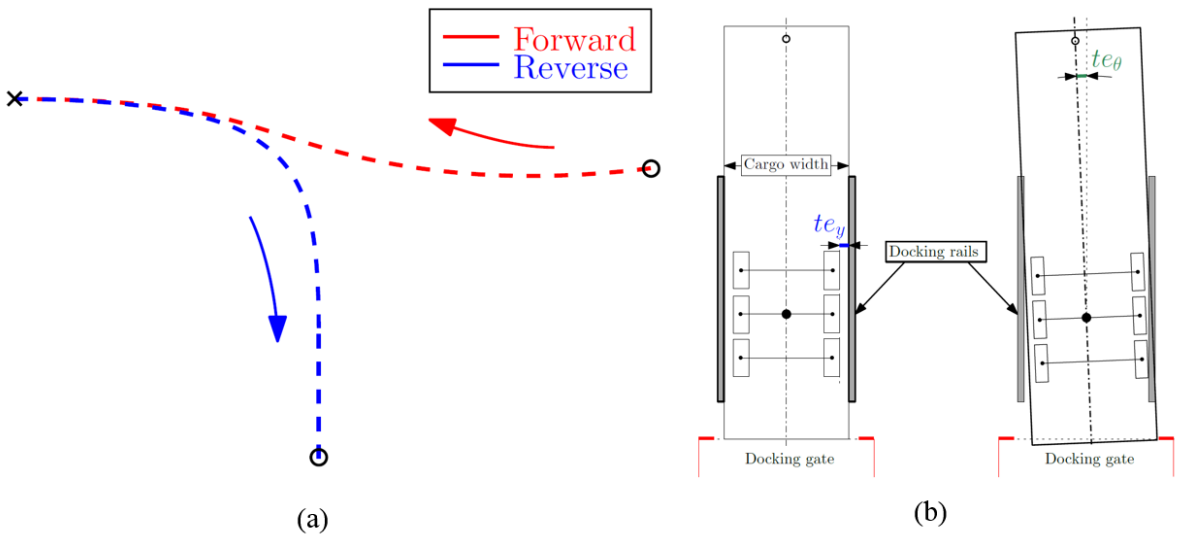

Figure 1: Schematically representing: (a) docking path (forward and reverse motion), (b) lateral and orientation tolerance at docking gates

By considering aforementioned points, a driver support system appears to be a good solution, where either the driver's spatial view can be enhanced or the docking maneuver can be performed while keeping the driver out-of-the-control-loop. Such a novel concept of a driver support system is described by Kural et al. (2016) for docking of articulated vehicles using an

unmanned aerial vehicle (UAV). This paper describes a path following controller which can be used to perform the docking maneuver.

2. System Description

A closed-loop control schematic of the entire system is presented in Figure 2. It can be observed from the schematic that there are mainly three components in the system: reference path, controller and vehicle model. The main objective of path following controller is to track the central turn point $U = [x_2, y_2, \theta_2]$ of the rear-most vehicle unit along the reference path at low speeds. However, steer axles are generally part of the prime-mover and not the trailing units, which brings to the two parts of controller, namely; driver model and steering translation. The driver model estimates the lateral error e_y using reference path R_{REL} and control point U and predicts a controller output δ^*. Inverse kinematics is used as steering translation technique, which translates the controller output (with respect to U) to actual required steering angle δ. The steering angle δ, together with longitudinal velocity of prime-mover drive axle v_0 are then fed as inputs to vehicle model.

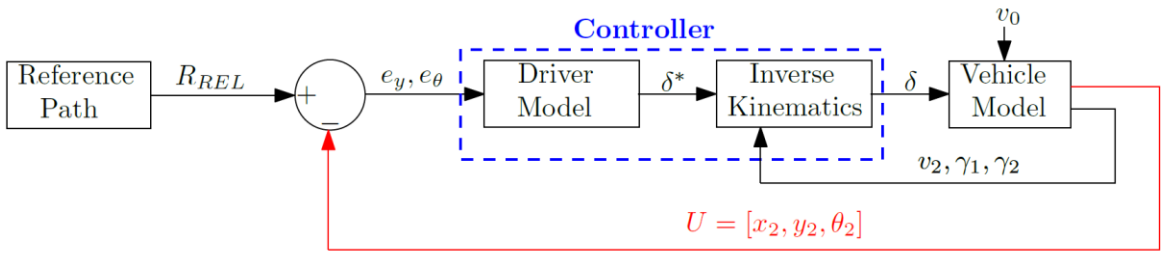

Figure 2 – Closed-loop control schematic of system

First, control problem is formulated in subsection 2.1, followed by a brief description of reference path in subsection 2.2, vehicle model in subsection 2.3 and inverse kinematics in subsection 2.4, respectively. The section is concluded with a description of an optimization routine for tuning the controller gains in section 2.5.

2.1 Control Problem Formulation

As discussed in section 1, the lateral error e_y and orientation error e_θ both are important for docking operation, therefore, to determine the controller output δ^*, the control goal is defined as presented in Equation (1).

$$\begin{bmatrix} e_y \\ e_\theta \end{bmatrix} \rightarrow 0 \; ; t \rightarrow \infty \tag{1}$$

A virtual tractor technique is used for the formulation of driver model as described by Morales et al. (2009), mainly due to the bi-directional operation of vehicle combination during docking maneuver. Due to this technique, rear-most unit of vehicle combination can be considered as virtual tractor and reverse motion problem can be treated as forward motion as the virtual tractor always aligns in the direction of motion (i.e. orientation = θ_2 (forward); orientation = $\theta_2 + \pi$ (reverse)). Initially, driver model estimates the lateral error e_y and orientation error e_θ using the central turn point U and relevant reference point R_{REL}. Driver model first creates a buffer of relevant reference points R_i and R_{REL} corresponds to the minimal of absolute distances between U and one of the reference points R_i, as schematically presented in Figure

3. R_{REL} is determined using Equation (2), where $\Delta x_i,\ \Delta y_i$ are positional errors between U and one of the relevant points R_i.

$$R_{REL} = argmin_{R_i} \sqrt{(\Delta x_i^2 + \Delta y_i^2)};\ \Delta x_i = \left(x_2 - x_{ref(i)}\right) \,\&\, \Delta y_i = (y_2 - y_{ref(i)}) \quad (2)$$

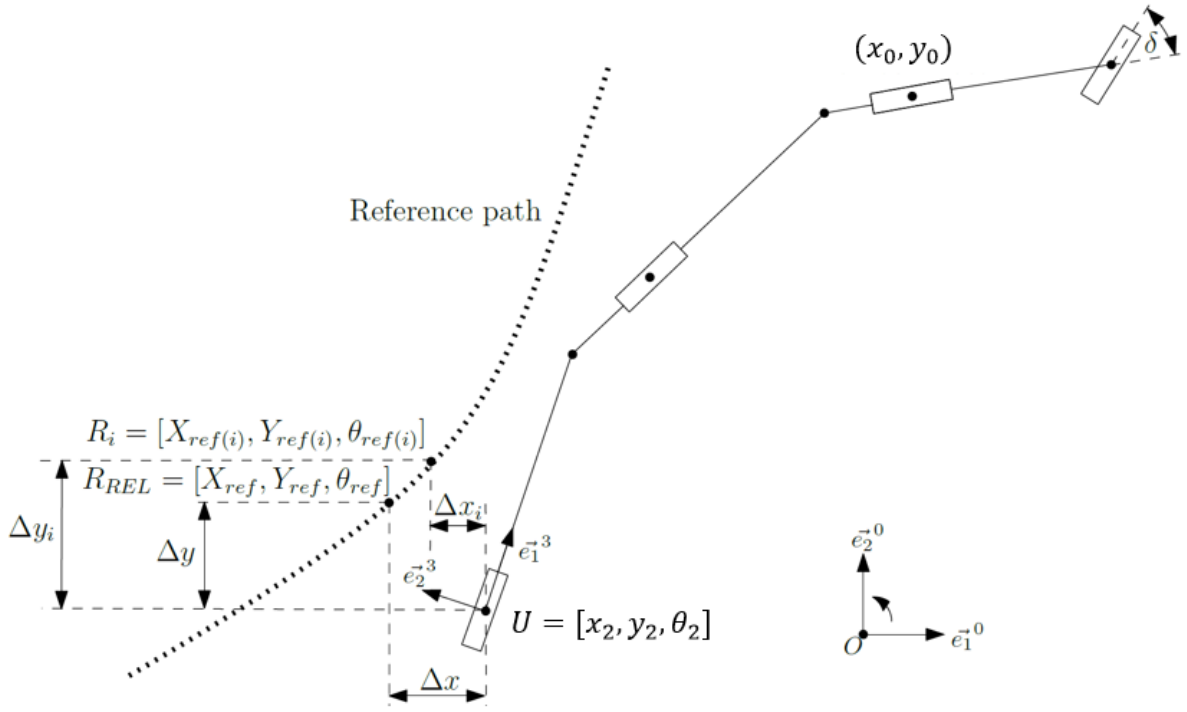

Figure 3: Estimation of lateral error e_y and orientation error e_θ

Once R_{REL} is determined, the lateral error can be calculated using positional errors $(\Delta x, \Delta y)$. However, the positional errors are defined in global coordinate system $e^{\rightarrow 0}$ which can be transformed into local coordinate system of rear-most vehicle unit $e^{\rightarrow 3}$ using orientation of rear-most vehicle unit θ_2. Thus, lateral error can be estimated as expressed in Equation (3).

$$e_y = \Delta y\, cos\theta_2 - \Delta x\, sin\theta_2\ ; \qquad \Delta x = \left(x_2 - x_{ref}\right) \,\&\, \Delta y = (y_2 - y_{ref}) \qquad (3)$$

The orientation error e_θ is defined as a difference between the orientation of R_{REL} and U, as expressed in Equation (4). The condition is applied to ensure the correct interpretation of error even when $e_\theta > \pi$.

$$e_\theta = \begin{cases} \theta_{ref} - \theta_2 & ;\ |\theta_{ref} - \theta_2| \le \pi \\ \theta_{ref} - \theta_2 - 2\pi sign(\theta_{ref} - \theta_2) & ;\ otherwise \end{cases} \qquad (4)$$

As described by Salvucci et al. (2004), human driver utilize two visual points (one near and one far point) for steering control to follow the reference path, which may result in both accurate and smooth path following, therefore, as presented in Figure 4, the controller projects two heading vectors $\underset{H_1}{\rightarrow}$, $\underset{H_2}{\rightarrow}$ from control point U using two look-ahead gains LG_1, LG_2, respectively. The look-ahead gains are nothing but controller parameters.

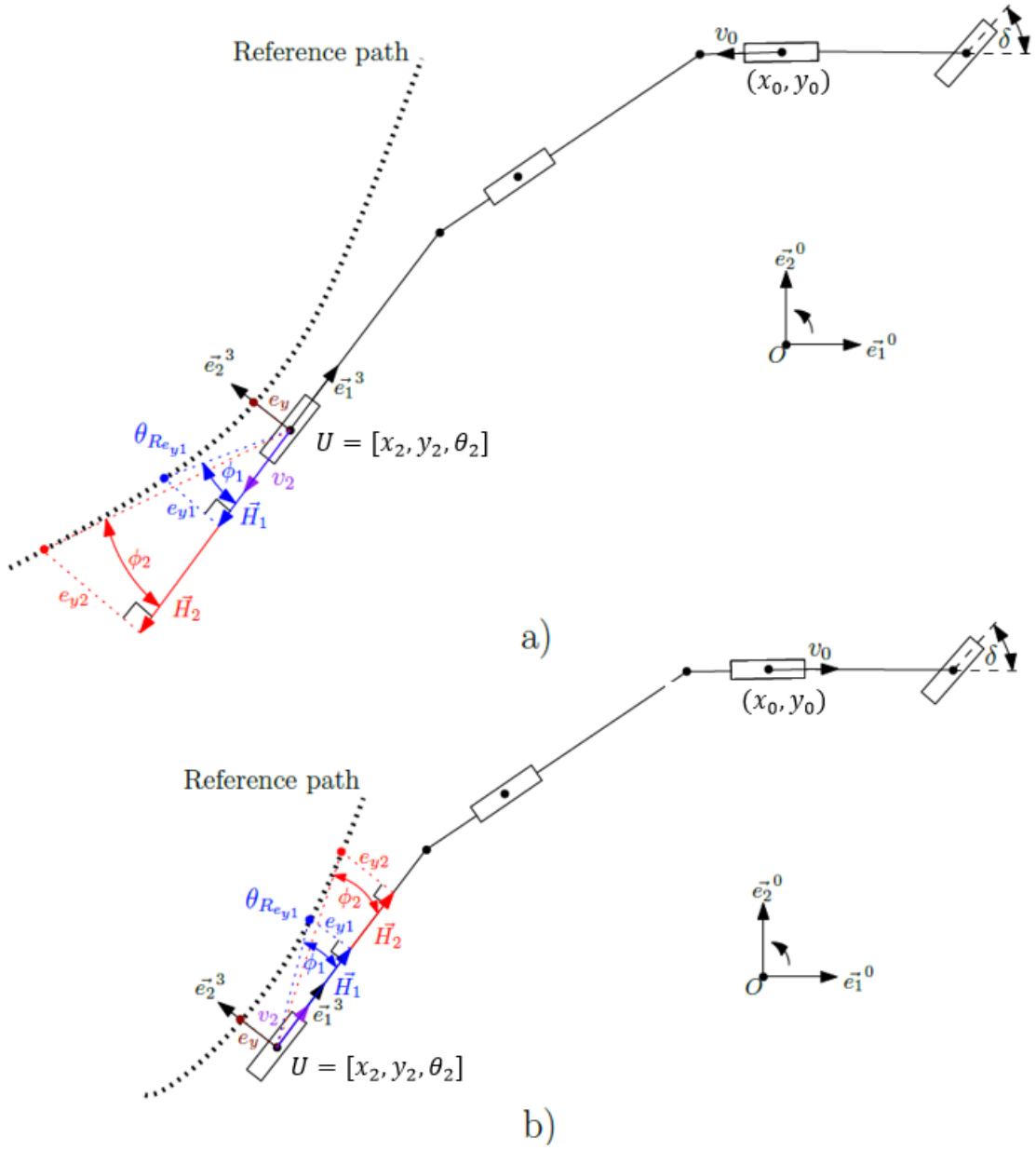

Figure 4: Schematic representation of correction angles φ_1, φ_2 corresponding to look-ahead gain 1 and 2, respectively: (a) reverse motion (b) forward motin

The heading vectors can be described as presented in Equation (5). Further, an orthogonal line is projected from the end of respective heading vectors on to the respective R_{REL}. The respective lateral e_{y1}, e_{y2} are estimated as presented in Equation (3). The correction angles φ_1, φ_2 can be obtained using Equation (6) corresponding to two look-ahead gains. The resultant correction angle φ is defined as a weighted average of the two correction angles as presented in Equation (7).

$$\left.\begin{aligned} \underset{H_1}{\rightarrow} &= sign(v_2)\, LG_1 \\ \underset{H_2}{\rightarrow} &= sign(v_2)\, LG_2 \end{aligned}\right\} \tag{5}$$

$$\left.\begin{aligned}\varphi_1 &= \tan^{-1}\left(\frac{e_{y1}}{|\overrightarrow{H_1}|}\right)\\ \varphi_2 &= \tan^{-1}\left(\frac{e_{y2}}{|\overrightarrow{H_2}|}\right)\end{aligned}\right\} \tag{6}$$

$$\varphi = w_1\,\varphi_1 + w_2\,\varphi_2 \tag{7}$$

Since, the heading vectors are defined using look-ahead gains, therefore, the weighing factors $w_1,\ w_2$ are also defined using look-ahead gains as presented in Equation (8).

$$\left.\begin{aligned}w_1 &= \frac{LG_1}{LG_1+LG_2}\\ w_2 &= 1 - w_1\end{aligned}\right\} \tag{8}$$

Finally, the controller output δ^* can be formulated similar to a PI controller using two controller gains K_s and K_I as presented in Equation (9).

$$\delta^* = K_s\,\varphi + K_I\,\int e_y\ dt \tag{9}$$

The steer sensitivity K_s can be considered as a proportional gain which is multiplied with resultant correction angle φ. This term is a dominant factor in compensating both the lateral and orientation error. K_I can be considered as an integral gain which is multiplied with integral of lateral errors. This term eliminates the steady state lateral error and due to the non-holonomic constraints of the vehicle model, it also eliminates e_θ.

2.2 Reference path

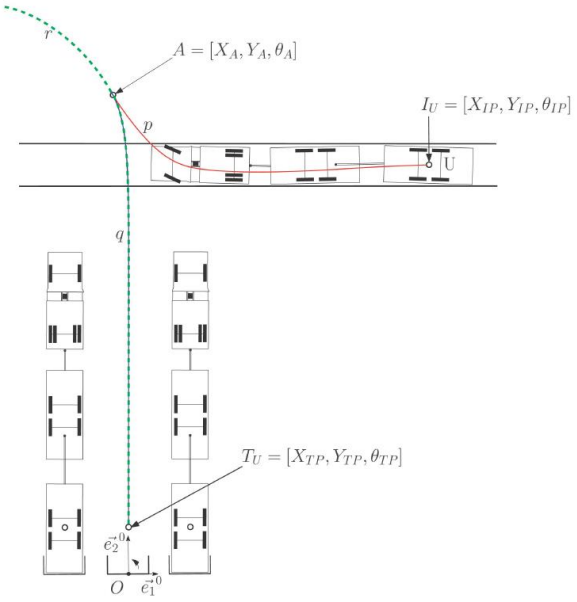

Figure 5: Schematic description of docking (reference) path

The reference path for docking maneuver is generated by path planner. The goal of the path planner is to minimize the travelled distance along the path while ensuring the kinematic viability of reference path. The path planner considers mainly 5 set of inputs: initial pose of control point $I_U = [X_{IP}, Y_{IP}, \theta_{IP}]$, terminal pose of control point $T_U = [X_{TP}, Y_{TP}, \theta_{TP}]$, vehicle

dimensions (such as wheel-bases, king-pin locations, rear overhang, track-widths), vehicle limitation (i.e. maximum steering angle) and available space constraint (i.e. road geometry). The docking path is generated in two steps, which are as follows:

- In first step, curve r as presented in Figure 5 is generated from terminal pose T_U. It is created by running the vehicle model in forward direction from T_U with constant longitudinal velocity of prime-mover drive axle v_0 and a steering angle profile with respect to time $[\delta, t]$.
- In second step, curve p as presented in Figure 5 is generated from initial pose I_U. It is created by Dubins curve, which is a curve of minimal length that connects two points in 2-D Euclidean plane $\boldsymbol{R^2}$ continuously. LaValle (2006) has also described Dubins curves as a solution to bounded-curvature shortest path problem. Therefore, transition point $A = [X_A, Y_A, \theta_A]$ corresponds to the minimum length of curve p.

The resultant docking path comprises forward motion from initial pose I_U to transition point A along curve p and reverse motion from transition point A to terminal pose T_U along curve q as presented in Figure 5.

2.3 Vehicle Model

The motion of articulated vehicles can be described using kinematic relations, where a vehicle combination can simply be represented by considering wheel-bases[1] of each vehicle unit and position of king-pin. A single-track model is used to describe these kinematic relations. A schematic of double articulated vehicle (DAV) is presented in Figure 6.

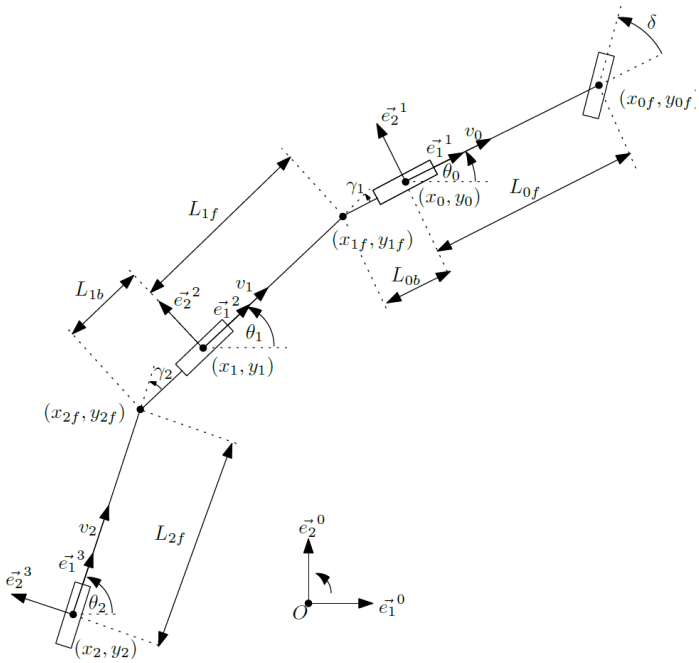

Figure 6 – Kinematic model of double articulated vehicle (DAV)

The global positions of vehicle axles ((x_{0f}, y_{0f}), (x_1, y_1), (x_2, y_2)) and king-pins ((x_{1f}, y_{1f}), (x_{2f}, y_{2f})) are defined with respect to a reference point (x_0, y_0) which is considered at the drive axle of prime-mover. The two main inputs describing motion of vehicle model are longitudinal velocity of prime-mover drive axle v_0 and steering angle δ. The wheel-base of prime-mover

[1] For articulated vehicle units, it is defined as distance between king-pin and rear axle of respective unit.

L_{0f}, wheel-bases of articulated units L_{1f}, L_{2f} and king-pin positions with respect to rear axle L_{0b}, L_{1b} are required to set the vehicle dimensions. L_{0b}, L_{1b} are considered negative if the king-pin is placed behind the respective rear axle. The yaw rates of vehicle units ($\dot{\theta}_0,\ \dot{\theta}_1,\ \dot{\theta}_2$) can be obtained by applying a non-holonomic constraint (NHC) on the vehicle axles. The constraint can be derived by utilizing the fact that there must not be any lateral velocity in axle local coordinate system. The yaw rate $\dot{\theta}_0$ of prime-mover can be derived by applying NHC at steer axle and the corresponding $\dot{\theta}_0$ is presented in Equation (10). Similarly, yaw rates $\dot{\theta}_1$, $\dot{\theta}_2$ of articulated vehicle units can be derived by applying NHC at rear axles of respective articulated units and the corresponding $\dot{\theta}_1$, $\dot{\theta}_2$ are presented in Equation (11), (12), respectively. The articulation angles γ_1, γ_2 is defined as the difference between the yaw angles of two vehicle units which are connected via respective king-pin, as presented in Equation (13). The longitudinal velocities of articulated vehicle units in their local body coordinate system v_1, v_2 can be defined as presented in Equation (14).

$$\left.\begin{aligned} &\dot{y_{of}}\cos(\theta_0+\delta)-\dot{x_{of}}\sin(\theta_0+\delta)=0\\ &(\dot{\theta_0})=\frac{v_0}{L_{0f}}\tan(\delta)\end{aligned}\right\} \quad (10)$$

$$\left.\begin{aligned} &\dot{y_1}\cos(\theta_1)-\dot{x_1}\sin(\theta_1)=0\\ &(\dot{\theta_1})=\frac{v_0}{L_{1f}}\sin(\gamma_1)+\frac{L_{0b}}{L_{1f}}\cos(\gamma_1)\ (\dot{\theta_0})\end{aligned}\right\} \quad (11)$$

$$\left.\begin{aligned} &\dot{y_2}\cos(\theta_2)-\dot{x_2}\sin(\theta_2)=0\\ &(\dot{\theta_2})=\frac{v_1}{L_{2f}}\sin(\gamma_2)+\frac{L_{1b}}{L_{2f}}\cos(\gamma_2)\ (\dot{\theta_1})\end{aligned}\right\} \quad (12)$$

$$\left.\begin{aligned} &\gamma_1=(\theta_0-\theta_1)\\ &\gamma_2=(\theta_1-\theta_2)\end{aligned}\right\} \quad (13)$$

$$\left.\begin{aligned} &v_1=v_0\cos(\gamma_1)-L_{0b}\,\dot{\theta}_0\sin(\gamma_1)\\ &v_2=v_1\cos(\gamma_2)-L_{1b}\,\dot{\theta}_1\sin(\gamma_2)\end{aligned}\right\} \quad (14)$$

Tomar (2018)[2] have further extended it into a generic kinematic description, which can be applied for vehicles having n-number of articulations.

2.4 Inverse Kinematics

It is used as a steering translation technique to convert the controller output δ^* into actual steering angle δ. The inverse kinematics for articulated vehicles can be described similar to kinematic model as presented in subsection 2.3, by considering the two following differences:

- First is the reference point which is considered at the axle of rear-most articulated unit.
- Second is the inputs to inverse kinematics, which are longitudinal velocity of rear-most articulated unit v_2, controller output δ^* and articulation angles $\gamma_1,\ \gamma_2$.

Inverse kinematically, the yaw rates of vehicle units ($\dot{\theta}_0,\ \dot{\theta}_1,\ \dot{\theta}_2$) can be obtained by applying non-holonomic constraint (NHC) on the respective vehicle axles. The yaw rate $\dot{\theta}_2$ of rear-most articulated unit can be derived by applying NHC at rear-most king-pin by considering a virtual steer axle and the corresponding $\dot{\theta}_2$ is presented in Equation (15). Similarly, yaw rates $\dot{\theta}_1,\ \dot{\theta}_0$ of vehicle units can be derived by applying NHC at rear axles of respective vehicle units and the corresponding $\dot{\theta}_1,\ \dot{\theta}_0$ are presented in Equation (16), (17), respectively. The longitudinal velocities of vehicle units in their local body coordinate system $v_1,\ v_0$ can be defined as presented in Equation (18).

[2] It is an internal document and is not available on internet.

$$\left.\begin{aligned} &\dot{y_{2f}}\cos(\theta_2+\delta^*)-\dot{x_{2f}}\sin(\theta_2+\delta^*)=0\\ &(\dot{\theta_2})=\frac{|v_2|}{L_{2f}}\tan(\delta^*)\end{aligned}\right\} \quad (15)$$

$$\left.\begin{aligned} &\dot{y_1}\cos(\theta_1)-\dot{x_1}\sin(\theta_1)=0\\ &(\dot{\theta_1})=\ \text{sign}(v_0)*\text{sign}(L_{1b})\left[-\frac{v_2}{L_{1b}}\sin(\gamma_2)+\frac{L_{2f}}{L_{1b}}\cos(\gamma_2)\left(\dot{\theta_2}\right)\right]\end{aligned}\right\} \quad (16)$$

$$\left.\begin{aligned} &\dot{y_0}\cos(\theta_0)-\dot{x_0}\sin(\theta_0)=0\\ &(\dot{\theta_0})=\ \text{sign}(v_0)*\text{sign}(L_{0b})\left[-\frac{v_1}{L_{0b}}\sin(\gamma_1)+\frac{L_{1f}}{L_{0b}}\cos(\gamma_1)\left(\dot{\theta_1}\right)\right]\end{aligned}\right\} \quad (17)$$

$$\left.\begin{aligned} &v_1=v_2\cos(\gamma_2)+L_{2f}\,\dot{\theta}_2\sin(\gamma_2)\\ &v_0=v_1\cos(\gamma_1)+L_{1f}\,\dot{\theta}_1\sin(\gamma_1)\end{aligned}\right\} \quad (18)$$

Only the magnitude of v_2 is considered in the Equation (15) due to the concept of virtual tractor. The sign of velocity v_0 is considered in Equation (16), (17) to make it applicable in both forward and reverse motion. The sign of L_{0b}, L_{1b} in Equation (16), (17) is considered mainly to incorporate the influence of king-pin position with respect to respective rear axle. However, the yaw rate of prime-mover $\dot{\theta}_0$ is already defined using kinematics as presented in Equation (10). Therefore, by equating Equations (10) and (17), the actual steering angle δ can be expressed using Equation (19).

$$\delta=\tan^{-1}\left[\text{sign}(v_0)*\text{sign}(L_{0b})*\frac{L_{of}}{v_0}\left(-\frac{v_1}{L_{0b}}\sin(\gamma_1)+\frac{L_{1f}}{L_{0b}}\cos(\gamma_1)\left(\dot{\theta_1}\right)\right)\right] \quad (19)$$

Tomar (2018) have further extended it into a generic inverse kinematic description, which can be applied for vehicles having n-number of articulations..

2.5 Optimization Routine

As mentioned in subsection 2.1, the controller require four controller gains, namely, steer sensitivity K_s, look-ahead gains LG_1, LG_2 and integral gain K_I which needs to be tuned for optimal path following performance. As presented in Figure 2, the reference path, direction of motion and vehicle model are part of the closed-loop, therefore, controller gain values would require optimization if either of the reference path, direction of motion or vehicle model (i.e. vehicle combination) is changed. Since, both the lateral error e_y and orientation error e_θ are considered important for docking operation, therefore, two cost functions CF_1, CF_2 are defined using mean square value of e_y and e_θ, respectively, as presented in Equation (20).

$$\left.\begin{aligned} &CF_1=\frac{1}{k}\left(\sum_{j=1}^{k}e_{yj}^2\right)\ ;\text{k}=\text{size}\ (\text{e}_{\text{yj}})\\ &CF_2=\frac{1}{k}\left(\sum_{j=1}^{k}e_{\theta j}^2\right)\end{aligned}\right\} \quad (20)$$

A forward section (curve p, see Figure 5) of docking path is used as reference path and a single articulated vehicle (SAV) is used in a three step optimization routine, which is required for tuning four controller gains. The three steps of optimization routine are as follows:

Step-1: K_s v/s LG_1

In this step, K_s and LG_1 are the only controller parameters which contribute to controller output. A range of K_s and LG_1 is selected and vehicle model is run for each combination of (K_s, LG_1) and respective cost function values are stored in a matrix. Using surfplots, an optimal range of K_s and LG_1 are selected, such a plot for CF_1 is presented in Figure 7. LG_1 is selected by minimizing the root mean square of respective cost function with respect to LG_1, such a plot

for this step is presented in Figure 8. During the optimization, CF_1 is considered as main cost function to minimize the lateral error, therefore, LG_1 is selection based on CF_1.

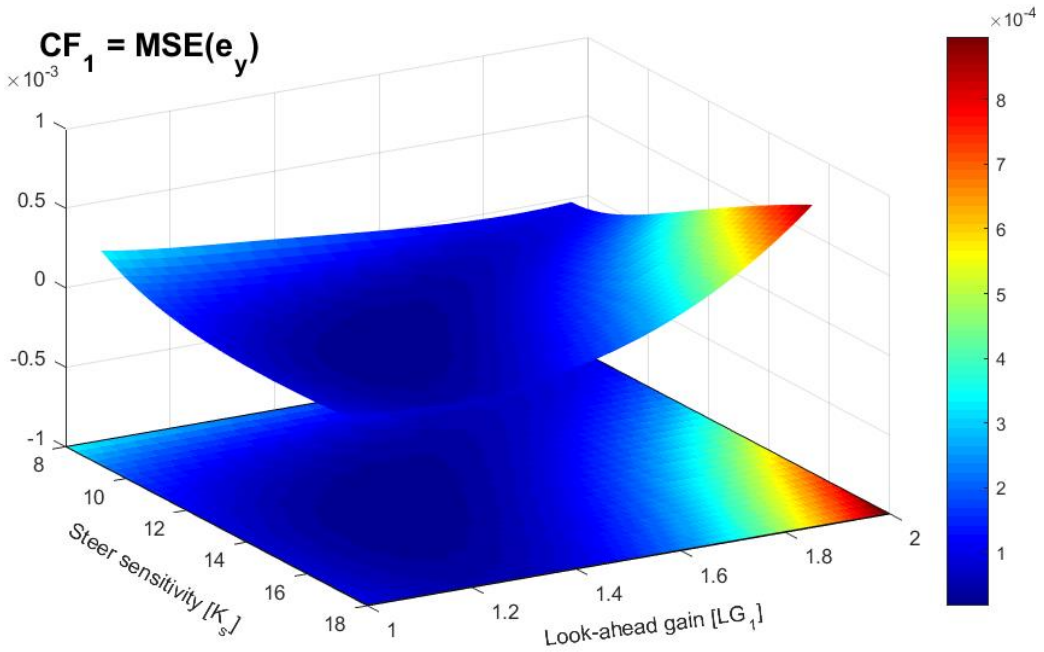

Figure 7: Surfplot of CF_1 (Step-1)

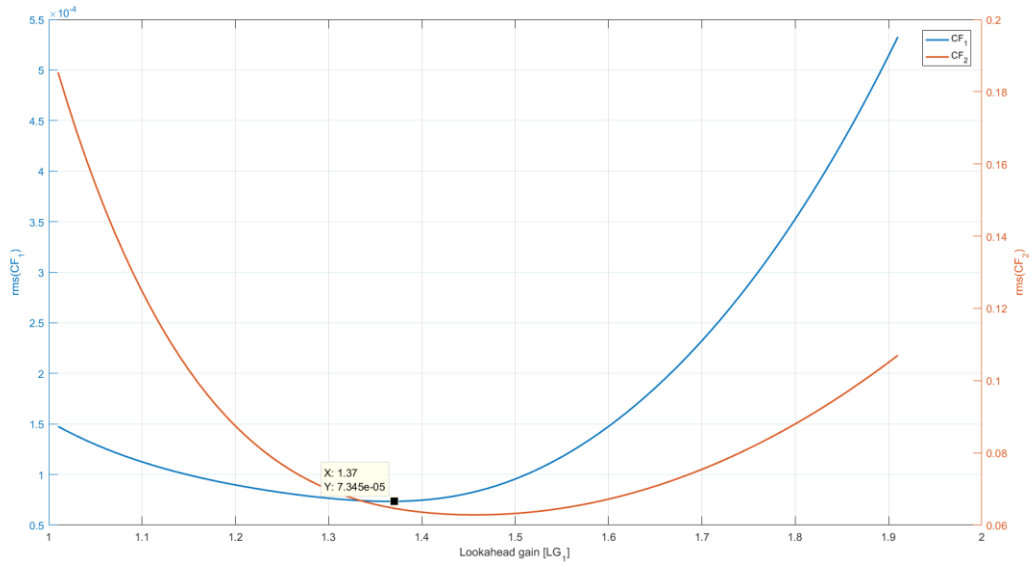

Figure 8: Root mean square of cost functions with respect to LG_1

Step-2: K_s v/s LG_2

In this step, second look-ahead gain LG_2 is added to controller. Similar approach as Step-1 is repeated in this step for a range of K_s and LG_2 while keeping the LG_1 same as selected in Step-1 and respective cost function values are stored in a matrix. LG_2 is selected using surfplots and by minimizing the root mean square of respective cost function with respect to LG_2.

Step-3: K_s v/s K_I

This is final step, in which integral gain K_I is also added to controller. Similar approach as the Step-1 is repeated in this step for a range of K_s and K_I (while keeping the LG_1 and LG_2 value constant according to previous two steps) and respective cost function values are stored in a matrix. K_s and K_I is selected using surfplots and by minimizing the root mean square of respective cost function with respect to K_s and K_I, respectively. This summarizes the optimization routine.

3. Results and Discussion

The controller is formulated as presented in Equation (9), however, the impact of each controller gain is not clear, therefore, three controller configurations are tested for SAV on same reference path. These controller configurations are selected based on the aforementioned optimization steps and are as follows:

- $K_s - LG_1$ (Step-1)
- $K_s - LG_1 - LG_2$ (Step-2)
- $K_s - LG_1 - LG_2 - K_I$ (Step-3)

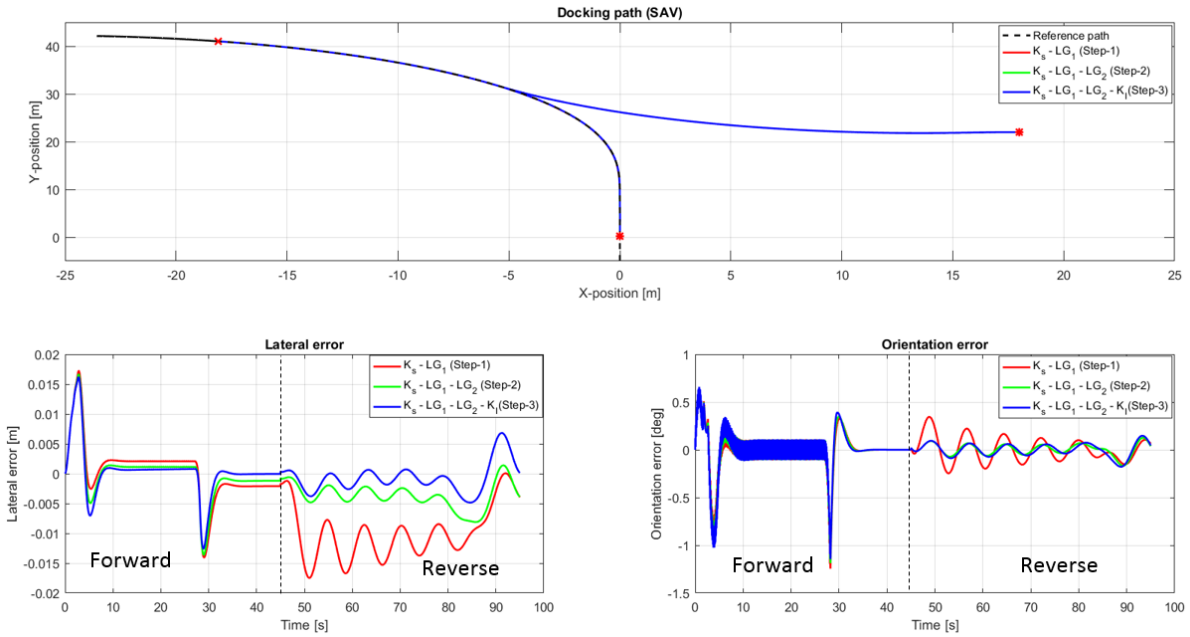

Figure 9: Contribution of controller gains during path following

The docking path, lateral error and orientation error for each controller configuration is presented in Figure 9. From the docking path and orientation error presented, it is very clear which controller configuration is best, however, from lateral error, it is clearly visible that the controller as formulated in Equation (9) performs best and is selected for further evaluation. Most improtantly, from both lateral and orientation error plot, it can be observed that both of them converges to zero in both forward and reverse motion, which provides a proof of concept.

To demonstrate the functionality of controller, a second level of proof of concept is generated using a scaled test setup. The test setup can be described by following points:

- The test vehicles are 1:14 scaled RC tractors and trailers from TAMIYA, which uses small servo motors for actuating steering and traction.

- A camera is used as a sensor (visual-GPS) to localize the test vehicle in the field of view. For localization, AR markers also known as ArUco markers are used in conjunction with OpenCV libraries.
- A XBEE PRO module is used for communication between control computer and micro-controller onboard the vehicles.

A docking maneuver is performed using scaled SAV (tractor-semitrailer) (i.e. $L_{2f} = L_{1b} = 0$) for the demonstration of controller functionality. The docking path, lateral error and orientation error are presented in Figure 10 for SAV.

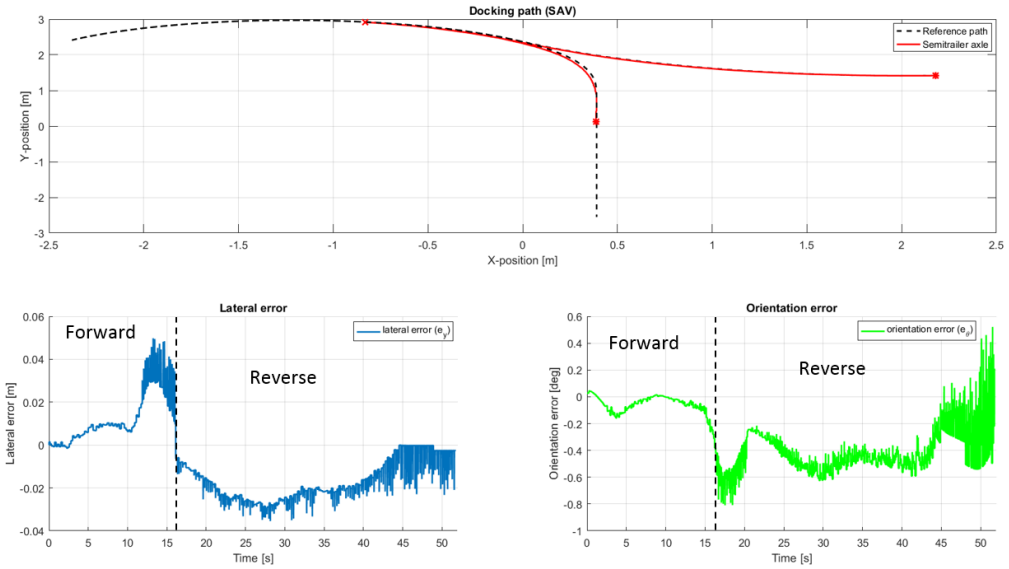

Figure 10: Path followed, lateral error and orientation error for scaled SAV

It is improtant to realize that the test vehicles are merely toys and not the real vehicles. The test vehicles have large mechanical plays due to plastic parts and even the actuators are simple servo motors which also exhibit significant amount of plays. These limitations of the test setup is the primary reason for observed path deviations together with controller gain parameters (as they were not tuned for the test vehicles). By considering this, it can be observed from the Figure 10, that the controller follows the reference path for SAV, which is the main objective and further, the lateral error and orientation error both are converging to zero and hence, satisfy the control goals.

4. Conclusion

Docking or parking of an articulated vehicle is cumbersome for majority of the human drivers, mainly arising from human limitation. A driver support system using a path following bi-directional controller presented as a feasible solution to this problem. The main goal of the controller is to track the control point (central turn point of rear-most articulated unit) along the reference path both in forward and reverse motion while converging the lateral and orientation error to zero. The controller satisfies this goal as shown by the simulation results presented in Figure 9. Further, to demonstrate the controller functionality in real world, it has been implemented in a scaled setup and docking maneuver is performed with scaled test vehicle, which also provides the same conclusion. Since, the controller presented is formulated as a path following controller, therefore, it is applicable in all of the scenarios where a reference path can be generated. Moreover, it has been proved that the functionality of controller is bi-

direction, which makes it compelling for multiple scenarios (other than docking). However, despite the satisfactory results, further research is needed in following areas:

- It is very clear that the path following performance is sensitive to controller gain values and the step-1 of optimization routine is difficult to execute because of unknown stability regions, which varies with the vehicle combination. Therefore, either the optimization routine should be performed using the stability analysis or an another optimization routine must be created.
- The controller gain values would require tuning with the change of reference path, vehicle or direction of motion, which require significant amount of time, therefore, further efforts should be directed to find correlations between the controller gain values with respect to reference path, vehicle combination or direction of motion.
- Validation of controller functionality through full scale vehicle testing.

References

- LaValle, S.M. (2006), Planning algorithms, Cambridge university press.
- Isiklar, G. (2007), "Simulation of complex articulated commercial vehicles for different driving maneuvers", Master's thesis, Eindhoven University of Technology.
- Kural, K., Besselink, I., Xu, Y., Tomar, A. and Nijmeijer, H. (2016), "A driver support system for improved maneuvering of articulated vehicles using an unmanned aerial vehicle" in HVTT14: International Symposium on Heavy Vehicle Transport Technology, Rotorua, New Zealand.
- Rakic, B., Stegeman, J. and Kind, M. (2011), "Monitoring Traffic Safety Longer and Heavier Vehicles", Ministry of Infrastructure and Environment, Arcadis, Hague.
- Tomar, A.S. (2018), "Kinematics of Articulated Vehicles", internal document, HAN Automotive Research, https://github.com/HAN-AR/INTRALOG-vehicle-models-controller/blob/master/docs/Articulated_vehicle.pdf.
- Odhams, A.M.C., Roebuck, R.L., Lee, Y.J., Hunt,S.W. and Cebon, D. (2010), "Factors influencing the energy consumption of road freight transport" in proceedings of the institution of Mechanical Engineers, part C: Journal of Mechinical Engineering Science, pp. 1995-2010.
- Salvucci, D.D. and Gray, R. (2004), "A two-point visual control model of steering", Perception, 33(10), pp. 1233-1248.